Method to compute atomic and molecular photoionization cross sections by use of basis sets

L. Veseth
Department of Physics, University of Oslo, 0316 Oslo 3, Norway
(Received 12 October 1990)

An alternative approach is presented to the problem of computing atomic and molecular photoionization cross sections by use of basis sets. The present method is based on a simple integral equation that relates the real polarizability on the imaginary frequency axis to the photoionization cross section. Hence the computational work consists in obtaining polarizabilities for imaginary frequencies. Many-body perturbation theory is used for that purpose, and the perturbation expansion is complete to second order in the Coulomb interaction. In that way there is a comprehensive inclusion of correlation effects. Techniques to invert the integral equation to obtain photoionization cross sections from the computed polarizabilities are discussed, and results are given for the atomic systems neon and argon as test cases.

I. INTRODUCTION

The development of accurate methods to compute atomic and molecular photoionization cross sections by use of basis sets (algebraic approximation) has been a long-standing problem in atomic and molecular physics. Sophisticated numerical techniques of current use in the atomic case are quite problematic for molecules due to the difficulties involved in obtaining accurate continuum orbitals for multicenter systems.

For light diatomic hydrides like CH, OH, and FH, single-center expansions have been found to provide a useful method for obtaining continuum orbitals of reasonable accuracy [1-4]. However, for molecules with several nuclei of approximately equal charge, the single-center approximation method is hardly of any interest.

Another problem in atomic and molecular photoionization calculations is that reliable predictions require a rather thorough inclusion of correlation effects in the initial, as well as the final, electronic state of the system. In the rather few molecular calculations that are available so far the emphasis has mainly been put on obtaining continuum orbitals, which means that the molecular results are normally on the Hartree-Fock level of accuracy. Various variational techniques are commonly used to derive the continuum orbitals in the molecular case [3-5].

The Stieltjes method [6-8] represents an algebraic approach to the problem which is somewhat different from the techniques mentioned above. By the Stieltjes method no explicit recourse is made to the continuum orbitals, and the continuum of the system is represented by a series of pseudostates obtained from general techniques in quantum chemistry. Although the Stieltjes method has been quite successful in several molecular cases [9, 10], it is still of considerable interest to work out different approaches to the difficult problem of computing atomic and molecular photoionization cross sections.

The present work presents an indirect algebraic approach with no explicit recourse to continuum orbitals, and which basically does not discriminate in any way between atomic and molecular systems. The feasibility of the method is, however, in the present discussion demonstrated only for the atomic systems neon and argon.

II. THEORY

A. Atomic and molecular polarizability

The dynamic polarizability $\alpha(\omega)$ represents the linear response of an atomic system to an external electric field, and is defined by the equation

$$\mathbf{p}=\alpha(\omega)\mathbf{F}\ , \tag{1}$$

where $\mathbf{p}$ is the electric dipole moment and $\mathbf{F}$ is the applied external field. The external field will be assumed to be of the form $F\cos(\omega t)$, directed along the space-fixed z axis, and the interaction with the external field adds a time-dependent perturbation given by

$$V_{\rm ex}(t)=F\cos(\omega t)\sum_{i=1}^{N} z_i=\tfrac{1}{2}(e^{i\omega t}+e^{-i\omega t})Fd_z\ . \tag{2}$$

The dynamic polarizability $\alpha(\omega)$ is expressed in terms of the eigenvalues E_k and eigenstates $|\Psi_k\rangle$ of the total zero-field Hamiltonian, and the polarizability of the state $|\Psi_n\rangle$ is given by [11]

$$\alpha(\omega)=-\sum_{k\ (\neq n)}|\left\langle\Psi_k\left|\sum_{i=1}^{N} z_i\right|\Psi_n\right\rangle|^2 \times\left\{\frac{1}{E_n-E_k-\omega}+\frac{1}{E_n-E_k+\omega}\right\}\ . \tag{3}$$

In the equation above the summation sign represents a sum over bound excited states, and an integral over continuum states. Hence a reliable computation of $\alpha(\omega)$ requires accurate knowledge of bound as well as continuum states of the total unperturbed Hamiltonian.

B. Determination of $\alpha(\omega)$ by many-body perturbation theory

In the present work the problem of computing dynamic polarizabilities will be attacked by use of many-body perturbation theory. The total zero-field Hamiltonian is then written as follows:

$$H=H_0+H' ,$$
$$H_0=\sum_{i=1}^{N}\left[-\tfrac{1}{2}\nabla_i^2-\frac{Z}{r_i}+V_i\right] , \tag{4}$$
$$H'=\sum_{i<j=1}^{N}\frac{1}{r_{ij}}-\sum_{i=1}^{N}V_i ,$$

where V_i represents appropriate single-particle potentials. To obtain an expression for $\alpha(\omega)$ the time-dependent wave function to first order in the external field strength F will be needed. According to the time-dependent linked-cluster many-body expansion [12, 13] the first order wave function $\Psi^{(1)}(t)$ of the ground state is obtained in the form

$$|\Psi^{(1)}(t)\rangle=e^{-iE_0t}(|\Psi_0\rangle+|\Psi_1^+\rangle\tfrac{1}{2}Fe^{i\omega t}+|\Psi_1^-\rangle\tfrac{1}{2}Fe^{-i\omega t}) , \tag{5}$$

where E_0 denotes the lowest eigenvalues of H_0 of Eq. (4), and $|\Psi_0\rangle$ denotes the ground state of the total zero-field Hamiltonian H. $|\Psi_1^+\rangle$ is obtained from a linked-cluster expansion in which there is just one interaction with the $e^{i\omega t}$ part of $V_{ex}(t)$ of Eq. (2), and an unlimited number of interactions with H' of Eq. (4). In a similar way $|\Psi_1^-\rangle$ refers to just one interaction with the $e^{-i\omega t}$ part of $V_{ex}(t)$.

The linked-cluster expansions for $|\Psi_1^{\pm}\rangle$ are, according to Kelly [12], given by

$$|\Psi_1^{\pm}\rangle=\sum_L\frac{1}{E_0-H_0\mp\omega}H'\cdots\frac{1}{E_0-H_0\mp\omega}d_z\cdots\times\frac{1}{E_0-H_0}H'|\Phi_0\rangle . \tag{6}$$

In the expansion above the interaction with d_z [cf. Eq. (2)] may occur in all positions relative to H', and in all denominators to the left of the interaction with d_z there is a term $\mp\omega$. $|\Phi_0\rangle$ denotes the ground state of the unperturbed Hamiltonian H_0 of Eq. (4). It is also to be noted that the states $|\Psi_1^{\pm}\rangle$ are frequency dependent, but time independent. The linked-cluster expansion of Eq. (6) with no interaction with d_z yields the correct expression for $|\Psi_0\rangle$.

The mean value of the electric dipole moment p for the state $|\Psi^{(1)}(t)\rangle$ is

$$\langle p\rangle=\frac{\left\langle\Psi^1(t)\left|-\sum_{i=1}^{N}z_i\right|\Psi^{(1)}(t)\right\rangle}{\langle\Psi^{(1)}(t)|\Psi^{(1)}(t)\rangle} , \tag{7}$$

and the polarizability $\alpha(\omega)$ is then in accordance with Eq. (1) given by

$$\alpha(\omega)=\frac{\left\langle\Psi_0\left|-\sum_{i=1}^{N}z_i\right|\Psi_1^+\right\rangle+\left\langle\Psi_0\left|-\sum_{i=1}^{N}z_i\right|\Psi_1^-\right\rangle}{\langle\Psi_0|\Psi_0\rangle} . \tag{8}$$

C. The shifted Hamiltonian

Other partitions of the Hamiltonian H than that of Eq. (4) are often useful in many-body expansions. In the present work the shifted or Epstein-Nesbet Hamiltonian [14, 15] will be given special attention. In this partition

$$H=\mathcal{H}_0+\mathcal{H}' \tag{9}$$

with

$$\mathcal{H}_0=\sum_{l=0}|\Phi_l\rangle\langle\Phi_l|H|\Phi_l\rangle\langle\Phi_l| ,$$
$$\mathcal{H}'=\sum_{k\neq l}\sum_{l=0}|\Phi_k\rangle\langle\Phi_k|H|\Phi_l\rangle\langle\Phi_l| , \tag{10}$$

and where $\{|\Phi_l\rangle\}$ is the complete set of eigenstates of H_0. Now,

$$\mathcal{H}_0|\Phi_l\rangle=|\Phi_l\rangle\langle\Phi_l|H|\Phi_l\rangle ,$$

and the eigenvalues of $\mathcal{H}_0$ are consequently shifted compared with those of H_0. Thus, if the linked-cluster expansion is based on the partition $H=\mathcal{H}_0+\mathcal{H}'$, the denominators will be shifted, and since $k\neq l$ in the expression for $\mathcal{H}'$ there will be no diagonal elements of $\mathcal{H}'$ in the linked-cluster expansion. The use of the shifted Hamiltonian actually leads to an all-order inclusion of some normally important classes of diagrams in a finite many-body expansion. Hence a comparison of the results obtained with the two different partitions yields valuable information on the importance of the neglected higher-order terms.

D. The generalized complex polarizability

The linear response of a physical system to an external perturbation is described by the generalized polarizability (or susceptibility) $\alpha(\omega)$ given by [16]

$$\alpha(\omega)=\int_0^{\infty}\alpha(t)e^{i\omega t}dt . \tag{11}$$

Here $\alpha(t)$ is a function of time which depends on the properties of the system, and which is finite for all positive values of t. ω may now be regarded as a complex variable, i.e., $\omega\rightarrow\omega+i\eta$, and it follows that $\alpha(\omega)$ is an analytic function in the upper half of the ω plane.

The theory of complex functions may now be used to derive some very general properties of the polarizability. First of all there are the Kramers-Kronig dispersion relations relating the real and imaginary parts of $\alpha(\omega)$ on the real axis ($\eta=0$),

$$\mathrm{Re}\alpha(\omega)=\frac{2}{\pi}\mathrm{P}\int_0^{\infty}\frac{\omega'\mathrm{Im}\alpha(\omega')}{\omega'^2-\omega^2}d\omega' ,$$
$$\mathrm{Im}\alpha(\omega)=-\frac{1}{\pi}\mathrm{P}\int_{-\infty}^{\infty}\frac{\mathrm{Re}\alpha(\omega')}{\omega'-\omega}d\omega' , \tag{12}$$

where P indicates that the Cauchy principal value of the integral is to be taken.

From the definition of $\alpha(\omega)$ [Eq. (11)] it follows that $\alpha(i\eta)$ is real, i.e., $\alpha(\omega)$ is real on the imaginary axis. It can also be proved [16] that $\alpha(i\eta)$ decreases monotonically from a positive value $\alpha(0)$ at $\eta=0$ to zero as $\eta\rightarrow\infty$.

Finally, there is an important relation between the real values of $\alpha(i\eta)$ and the imaginary part $\mathrm{Im}\alpha(\omega)$ on the real axis,

$$\alpha(i\eta)=\frac{2}{\pi}\int_0^\infty \frac{\omega\,\mathrm{Im}\alpha(\omega)}{\eta^2+\omega^2}d\omega\ . \tag{13}$$

The cross section of photoionization $\sigma(\omega)$ is given by $\mathrm{Im}\alpha(\omega)$ through the well-known relation [11]

$$\sigma(\omega)=\frac{4\pi}{c}\omega\,\mathrm{Im}\alpha(\omega)\ , \tag{14}$$

and inserting $\sigma(\omega)$ in Eq. (13) we have

$$\alpha(i\eta)=\frac{c}{2\pi^2}\int_0^\infty \frac{\sigma(\omega)}{\eta^2+\omega^2}d\omega\ . \tag{15}$$

In the present work values of the photoionization cross section $\sigma(\omega)$ will be derived from the relation above.

From the Kramers-Kronig relations of Eq. (12) we obtain by use of Eq. (14)

$$\mathrm{Re}\alpha(\omega)=\frac{c}{2\pi^2}P\int_0^\infty \frac{\sigma(\omega')}{\omega'^2-\omega^2}d\omega'\ , \tag{16}$$

so that knowledge of $\sigma(\omega)$ enables a subsequent computation of $\mathrm{Re}\alpha(\omega)$. Furthermore, for a dilute gas containing N atoms (or molecules) per unit volume the index of refraction $n(\omega)$ is given by the approximate relation [17]

$$n(\omega)\approx 1+2\pi N\,\mathrm{Re}\alpha(\omega)\ . \tag{17}$$

E. Diagrammatic representation of $\alpha(\omega)$

To compute $\alpha(\omega)$ from Eqs. (6) and (8) we first of all have to make a choice of single-particle potentials V_i so that single-particle states $\varphi_n(\mathbf{r}_i)$ and orbital energies ε_n can be obtained from the single-particle Schrödinger equation

$$(-\tfrac{1}{2}\nabla_i^2-\frac{Z}{r_i}+V_i)\varphi_n(\mathbf{r}_i)=\varepsilon_n\varphi_n(\mathbf{r}_i)\ . \tag{18}$$

In the present investigation the single-particle wave functions will be represented by analytic expansions in terms of a finite set of known basis functions. This means that the continuum is described by a finite set of virtual orbitals. The Hartree-Fock potentials will be the present choice of single-particle potentials V_i, and the virtual orbitals are then based on the so-called V^N type of potentials.

Equations (6) and (8) enable a simple diagrammatic representation of $\alpha(\omega)$. In the lowest-order diagram there are no interactions with H' either in $|\Psi_0\rangle$ or in $|\Psi_1^{\pm}\rangle$. The corresponding diagram which represents the Hartree-Fock approximation to $\alpha(\omega)$ is shown in Fig. 1(a), and the contribution is

$$\alpha^{(0)}(\omega)=-\sum_{p,i}|\langle i|z|p\rangle|^2\times\left[\frac{1}{\varepsilon_p-\varepsilon_i-\omega}+\frac{1}{\varepsilon_p-\varepsilon_i+\omega}\right]\ . \tag{19}$$

Here p indicates occupied single-particle states, and i excited (virtual) states.

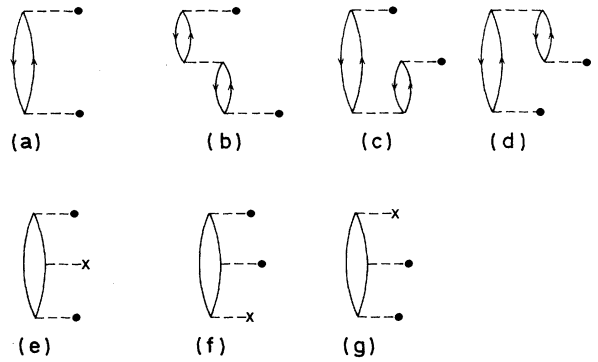

FIG. 1. Zero- and first-order diagrams contributiong to $\alpha(\omega)$. The heavy dot indicates interaction with the dipole operator (see text). Diagrams (e)–(g) occur with all possible arrow directions on the lines.

In the next order of approximation we have the corrections involving one interaction with H', and the corresponding first-order diagrams are shown in Figs. 1(b)–1(g). In Figs. 1(e)–1(g) the cross represents matrix elements of the form

$$\sum_{n=1}^{N}\langle an|0|bn\rangle-\langle a|V|b\rangle\ , \tag{20}$$

where

$$0=(1-P_{12})\frac{1}{r_{12}}\ , \tag{21}$$

and where P_{12} is the operator which permutes the coordinates of electrons 1 and 2. Thus with a Hartree-Fock potential all diagrams containing an interaction represented by a cross will vanish for closed-shell systems.

The relation between many-body theory and Hartree-Fock theory has been investigated by Chang, Pu, and Das [18] in the case of the static polarizability ($\omega=0$). They found that the contributions from the diagrams of Figs. 1(b)–1(d) are all included by the coupled Hartree-Fock method. Thus the perturbation expansion has to be carried to higher orders to include true correlation effects in the static case.

Some typical diagrams containing two interactions with H' are shown in Fig. 2. Terms involving two interactions with H' are referred to as second-order corrections, and a complete list of diagrams to this order is found in the monograph by Wilson [14]. A complete list of second-order diagrams like those of Fig. 2 actually contains 38 distinct diagrams for closed-shell systems.

All diagrams like those shown in Fig. 2 were included in the present investigation, i.e., a total of 38 distinct second-order diagrams in addition to the lower-order diagrams of Fig. 1. Using basis sets to represent the single-particle states the computation of any diagram is in principle straightforward.

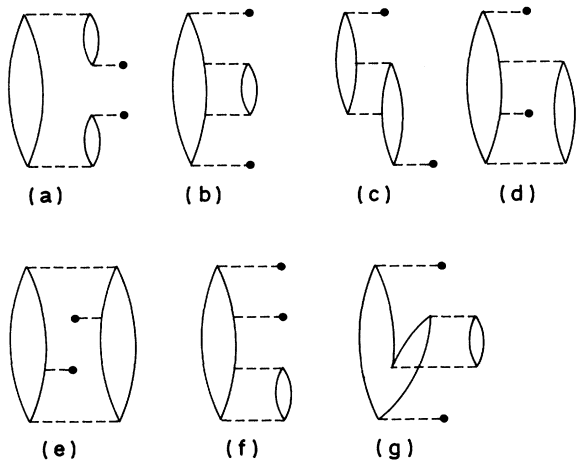

FIG. 2. Examples of second-order diagrams contributing to $\alpha(\omega)$ (arrows on the lines omitted). There is a total of 38 such distinct second-order diagrams for closed-shell systems.

F. Computation of photoionization cross sections

From the computed many-body values of $\alpha(i\eta)$ it is possible to invert the integral equation of Eq. (15) to obtain the photoionization cross section $\sigma(\omega)$. Equation (15) is an example of a Fredholm integral equation of the first kind. The standard method to invert this type of equation is to expand $\sigma(\omega)$ in a set of known basis functions $\psi_n(\omega)$, which in principle should be a complete set for the interval $(0,\infty)$ [19]. In practice a finite expansion with N terms has to be used, and we assume

$$\sigma(\omega)=\sum_{n=1}^{N} a_n\psi_n(\omega) \ . \tag{22}$$

Inserting Eq. (22) in Eq. (15) we obtain

$$\alpha(i\eta)=\frac{c}{2\pi^2}\sum_{n=1}^{N} a_n g_n(\eta) \ , \tag{23}$$

with

$$g_n(\eta)=\int_0^{\infty}\frac{\psi_n(\omega)}{\eta^2+\omega^2}d\omega \ . \tag{24}$$

The set of functions $g_n(\eta)$ is in the next step orthonormalized by the Gram-Schmidt procedure, and Eq. (23) is reexpressed in terms of the new orthonormal set of functions. It is then in principle easy to find the set of coefficients a_n, and the problem is solved.

To make this method of solution work in practice we need to find a set of linearly independent functions $\psi_n(\omega)$ which represents $\sigma(\omega)$ rather well so that the series of Eq. (22) can be terminated after a few terms. Otherwise the set of functions $g_n(\eta)$ of Eq. (23) may turn out to be nearly linearly dependent, with the consequence of no unique solution for the set of coefficients a_n. From Eq. (24) it follows that to avoid a singularity at the origin the functions $\psi_n(\omega)$ should tend to zero for $\omega\rightarrow 0$ faster than ω^2. On the other hand it is known that $\sigma(\omega)\rightarrow 0$ as $\omega\rightarrow\infty$. These requirements are fulfilled by the choice

$$\psi_n(\omega)=\omega^l e^{-k_n\omega} \ , \tag{25}$$

where l is an integer larger than two, and k_n is a positive constant. To ensure linearly independent functions the constants k_n may be selected according to the simple relation

$$k_n=k_0 C^{n-1} \ , \tag{26}$$

where C is a real constant larger than one.

An alternative way to determine the coefficients a_n of Eq. (23) is to carry out a least-squares fit to computed values of $\alpha(i\eta)$ for a series of discrete η values. The method of least-squares fitting also yields the covariance matrix for the coefficients a_n, and hence a valuable test of the linear independence of the functions $g_n(\eta)$.

By the present method $\sigma(\omega)$ (or actually the coefficient of photoabsorption) will obviously be obtained in the form of a smooth curve in the frequency range $\omega=0$ to ∞. Hence there will be no abrupt rise from zero to a finite value at the ionization threshold, but a reasonable solution should show a steep increase in $\sigma(\omega)$ around that frequency. The computation of $\alpha(i\eta)$ is in principle unproblematic since there are no poles on the imaginary axis, and a fast improvement in the rate of convergence of the many-body expansion for $\alpha(i\eta)$ is to be expected with increasing η.

III. COMPUTED RESULTS

A. Polarizabilities of the neon and argon atoms

Computed results for the closed-shell atoms neon and argon will be presented in this section. These atoms have been selected since they are complex enough to yield reasonable tests of the present basis set method on real many-particle systems, but small enough to avoid disturbing relativistic effects. In both cases extensive and accurate measurements are available, as well as computed results based on the sophisticated numerical techniques that have been developed for atomic systems.

The aim of the present investigation is not to improve on the theoretical results available in the literature, but rather to see whether the present indirect method to compute $\sigma(\omega)$ can compete with numerical methods involving explicit use of continuum orbitals. The next step will then be to apply the method to other systems, e.g., diatomic molecules, where current atomic methods are inapplicable due to the difficulties involved in obtaining accurate continuum orbitals.

The basis sets used for the present atomic calculation are extensions of the sets of Slater orbitals with optimized exponents published by Clementi and Roetti [20]. The extensions consist in inclusion of several extra diffuse s and p orbitals, which are more important for polarizability calculations than they are for energy optimization. In addition a rather large set of excited d orbitals will be required.

In the case of neon the $6s$, $4p$ basis of Clementi and Roetti was extended by three diffuse $2s$ Slater orbitals with exponents $\zeta=0.5$, 0.8, and 1.3, respectively. The p basis was extended by two extra diffuse $2p$ orbitals with

TABLE I. Computed values of $\alpha(i\eta)$ (in a.u., 1 a.u.=0.1482 Å^3) for the ground state of Ne.

	Standard Hamiltonian, Eq. (4)—order				Shifted Hamiltonian, Eq. (10)—order			
η	0	1	2	Total	0	1	2	Total
0.00	1.908	0.265	0.296	2.469	2.361	−0.135	0.401	2.627
0.25	1.861	0.231	0.260	2.352	2.268	−0.150	0.356	2.474
0.50	1.738	0.153	0.184	2.075	2.042	−0.173	0.263	2.132
1.00	1.402	0.004	0.057	1.463	1.524	−0.177	0.119	1.466
1.50	1.099	−0.071	0.008	1.036	1.122	−0.147	0.054	1.030
2.00	0.864	−0.096	−0.008	0.760	0.845	−0.115	0.027	0.758
3.00	0.560	−0.093	−0.010	0.457	0.518	−0.070	0.010	0.457
4.00	0.387	−0.076	−0.006	0.305	0.345	−0.045	0.005	0.306
6.00	0.212	−0.047	−0.002	0.163	0.184	−0.023	0.002	0.164
8.00	0.132	−0.031	−0.001	0.100	0.113	−0.013	0.001	0.101
10.00	0.090	−0.022	−0.000	0.068	0.076	−0.009	0.001	0.069

exponents $\zeta=0.7$ and 1.0, respectively. A set of six even tempered $3d$ Slater orbitals were used to describe the excited d orbitals, and the exponents were obtained from the relation [14]

$$\zeta_n=\zeta_0 R^{n-1} . \tag{27}$$

For neon a reasonable spread of the $3d$ orbital energies was obtained by the choice $\zeta_0=0.5$ and $R=1.6$.

For argon the $7s$, $5p$ basis set of Clementi and Roetti was extended by two diffuse $3s$ orbitals with exponents $\zeta=0.80$ and 1.45, respectively, and two extra diffuse $3p$ orbitals ($\zeta=0.5$ and 0.9) were added to the p basis. A basis set of five $3d$ orbitals with $\zeta_0=0.5$ and $R=1.9$ [cf. Eq. (27)] was used in this case. All excited states were computed in the Hartree-Fock potential of the neutral system, i.e., a V^N type of potential was used.

Values of the real polarizability $\alpha(i\eta)$ on the imaginary axis were computed at about 25 different η values in the range $n=0.0$ to 12.0 (in a.u.). The many-body expansions used to compute $\alpha(i\eta)$ were for these closed-shell systems complete to second order in the interaction with the Coulomb term H' [cf. Eq. (4)] or $\mathcal{H}'$ [cf. Eq. (10)]. Computations were carried out according to the shifted Hamiltonian of Eq. (10) as well as to the standard partition of Eq. (4).

The results obtained are presented for some selected η values in Tables I and II. Zero order refers to the diagram of Fig. 1(a), whereas first order refers to the diagrams of Figs. 1(b)–1(d) (one interaction with H' or $\mathcal{H}'$). In a similar way second order refers to the contribution from all the diagrams involving two interactions with H' or $\mathcal{H}'$, a few of which are shown in Fig. 2.

From the results of Tables I and II it is clear that the significance of the second-order contributions to $\alpha(i\eta)$ is greatly reduced for increasing η values in all cases. Another indication of the enhanced rate of convergence for increasing values of η is the fact that the discrepancy between the total results obtained with the standard and shifted Hamiltonians is also greatly reduced as η is increased.

The errors introduced by the finite basis set are difficult to estimate, but several test runs for various basis sets indicate that the errors that stem from the basis are probably smaller than those arising from the termination of the perturbation expansion. The present computed static polarizabilities ($\eta=0$) can be compared with experimental values and other theoretical predictions. In the case of Ne the experimental value is 2.67 a.u. [21], whereas the best current theoretical prediction seems to be the coupled cluster value of 2.70 a.u. [22]. The agreement with

TABLE II. Computed values of $\alpha(i\eta)$ (in a.u.) for the ground state of Ar.

	Standard Hamiltonian, Eq. (4)—order				Shifted Hamiltonian, Eq. (10)—order			
η	0	1	2	Total	0	1	2	Total
0.00	9.502	−0.195	0.244	9.558	12.88	−5.46	2.75	10.17
0.30	8.636	−0.565	−0.015	8.057	10.75	−4.31	1.83	8.273
0.60	6.849	−1.015	−0.246	5.584	7.338	−2.55	0.789	5.583
1.00	4.692	−1.109	−0.235	3.350	4.317	−1.20	0.250	3.362
1.50	2.971	−0.878	−0.144	1.950	2.457	−0.550	0.063	1.970
2.00	1.993	−0.645	−0.091	1.257	1.559	−0.299	0.009	1.269
3.00	1.053	−0.362	−0.049	0.642	0.786	−0.125	−0.014	0.646
4.00	0.648	−0.225	−0.031	0.392	0.476	−0.068	−0.014	0.394
6.00	0.320	−0.108	−0.016	0.197	0.236	−0.030	−0.009	0.198
8.00	0.195	−0.063	−0.009	0.122	0.145	−0.017	−0.006	0.123
10.00	0.133	−0.041	−0.006	0.086	0.100	−0.012	−0.004	0.086

TABLE III. The total computed photoionization cross section (Mb) of neon as a function of the photon energy ω.

ω (a.u.)	Standard Hamiltonian, Eq. (4)	Shifted Hamiltonian, Eq. (10)	Expt. [26]
0.80	5.68	6.21	6.34
0.90	6.97	7.40	7.71
1.00	7.98	8.28	8.47
1.20	9.22	9.13	8.96
1.60	9.47	8.57	8.40
2.00	8.35	7.13	7.40
2.50	6.71	5.64	6.22
3.00	5.23	4.65	5.25
4.00	2.97	3.44	3.70
5.00	1.62	2.57	2.49
6.00	0.91	1.89	1.71
7.00	0.53	1.34	1.22
8.00	0.33	0.92	0.86
9.00	0.21	0.61	0.64
10.00	0.13	0.39	0.49

the results presented in Table I is thus quite good, in particular for the value obtained with the shifted Hamiltonian. The recommended value of the static polarizability for argon is 11.07 a.u. [23], which is about 10% larger than the computed values of Table II.

The second-order corrections to $\alpha(i\eta)$ are of particular importance for the smaller η values, and they are in some cases seen to be numerically larger than the first-order contributions. There are significant second-order contributions from all the different types of diagrams shown in Fig. 2. A somewhat astonishing observation was that triple excitation diagrams like that of Fig. 2(g) are of great importance in all cases. Such rather large second-order terms may stem from the use of the V^N potential.

In many-body calculations of atomic polarizabilities for closed-shell systems all contributions beyond the lowest order are generally interpreted as correlation corrections. However, the results of Tables I and II demonstrate that the computed values to the lowest order as well as those of the next orders are strongly dependent on the chosen partitioning of the total Hamiltonian. Furthermore, preliminary results obtained with V^{N-1} type of single-particle potentials indicate that the role of correlation is heavily dependent on the choice of single-particle model. A similar conclusion was also made by Amusia and Cherepkov [24]. Hence, by the present method it seems hard to make a fruitful distinction between single-particle effects and correlation corrections. The challenge is certainly to have a perturbation expansion that includes both types of effects in the final answer in a sufficient manner.

B. The photoionization cross sections of neon and argon

Photoionization cross sections were obtained from Eq. (15) by use of the computed values of $\alpha(i\eta)$. This integral equation which links $\alpha(i\eta)$ and $\sigma(\omega)$ was inverted as described in Sec. II F. The crucial point in this process is an appropriate choice of the set of basis functions $\psi_n(\omega)$ of Eq. (22). These basis functions were chosen according to Eqs. (25) and (26), with $l=3$. The selection of the number of basis functions and the parameters k_0 and C of Eq. (26) is a matter of some trial and error. Generally the number of basis functions $\psi_n(\omega)$ should be kept as low as possible to avoid linear dependence among the functions $g_n(\eta)$ of Eqs. (23) and (24). The best criterion for a suc-

TABLE IV. The total computed photoionization cross section (Mb) of argon as a function of the photon energy ω.

ω (a.u.)	Standard Hamiltonian, Eq. (4)	Shifted Hamiltonian, Eq. (10)	Expt. [26]
0.60	25.29	24.09	31.1
0.70	31.68	29.15	36.3
0.80	33.86	30.69	36.3
0.90	32.08	29.02	33.5
1.00	27.45	25.11	28.9
1.20	14.96	14.83	17.1
1.40	4.51	6.25	5.70
1.60	0.00	1.57	1.54
1.80		0.22	0.91
2.00		0.75	1.18

cessful solution of Eq. (23) seems to be that the computed values of $\sigma(\omega)$ are stable within reasonable variations of the parameters k_0 and C of Eq. (26). To search for the best possible solution of Eq. (23) is obviously also an important criterion for the final choice of the parameters of the basis functions. The best solution was defined as the one that minimized the mean square deviation between the left- and right-hand sides of Eq. (23) for the discrete set of computed values of $\alpha(i\eta)$.

Computed values of the photoionization cross section $\sigma(\omega)$ are given in Tables III and IV and visualized in Figs. 3 and 4. Values of $\alpha(i\eta)$ were computed at about 25 different values of η in the range $\eta=0.0$ to 12.0 a.u., and the discrete values of $\alpha(i\eta)$ were fitted to a linear combination of exponentials to obtain a smooth and continuous representation of the function $\alpha(i\eta)$. A set of five basis functions $\psi_n(\omega)$ was used for neon as well as for argon. For neon the selection of parameters of Eq. (23) was $k_0=0.75$ and $C=2.0$, and for argon $k_0=2.20$ and $C=\sqrt{2}$. The different choices of parameters for Ne and Ar reflects the different shapes of the $\sigma(\omega)$ curves in the two cases. For Ar $\sigma(\omega)$ falls to nearly zero already at photon energies of about 1.7 a.u., whereas for Ne the curve extends to much higher photon energies, requiring a wider range of exponentials for an appropriate representation.

Photoionization cross sections based on the standard Hamiltonian of Eq. (4) as well as on the shifted Hamiltonian of Eq. (10) are given in Tables III and IV. The disparity that exists between the results obtained with the two different Hamiltonians indicates that the convergence of the perturbation expansion of $\alpha(i\eta)$ is still not complete, even with two interactions with the Coulomb part included. With the shifted Hamiltonian several classes of low-order diagrams will be included to all orders, and the shifted Hamiltonian tends to yield the best agreement with experiment for both neon and argon. This conclusion is in accordance with other many-body results on dynamic polarizabilities and photoionization [12, 25].

In Figs. 3 and 4 the present results obtained with the shifted Hamiltonian are compared with experimental values [26], and with the results of the R-matrix calculations of Burke and Taylor [27]. The R-matrix calculations seem to be representative for the best current theoretical methods, and only those results have been included in the present work for comparison. Many other important references to computations on Ne and Ar are found in the work of Burke and Taylor [27]. The pioneering calculations of Amusia, Cherepkov, and Chernysheva [28] using the random-phase approximation with exchange (RPAE), and the many-body perturbation theory (MBPT) results of Kelly and Simons [29] in particular also need to be mentioned. As stated earlier, the objective of the present work is not to improve on existing theoretical predictions for Ne and Ar, but rather to test a new method which should hold the promise of a wider range of applicability. The results shown in Figs. 3 and 4 indicate that the present approach is a competitive alternative to existing methods even for the simple atomic systems Ne and Ar. The agreement with experiment is in the case of Ar seen to be somewhat inferior to the excellent one for Ne. The reason for that is probably related to the somewhat poorer prediction of the static polarizability in Ar, which in turn seems to stem from an insufficient convergency of the perturbation expansion.

Dispersion curves $[\alpha(\omega)]$ obtained from Eq. (16) and the computed values of $\sigma(\omega)$ are shown in Figs. 5 and 6. The most characteristic feature of the dispersion curves is

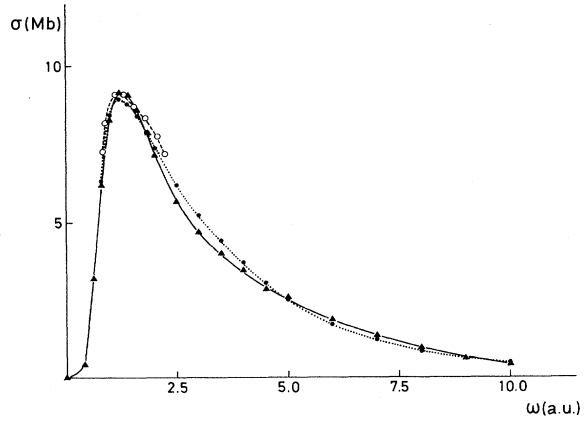

FIG. 3. Computed total photoionization cross section of neon. ▲–▲–▲, present results; ○––○––○, R-matrix results of Burke and Taylor [27] (length form); ●––●––●, experiment [26].

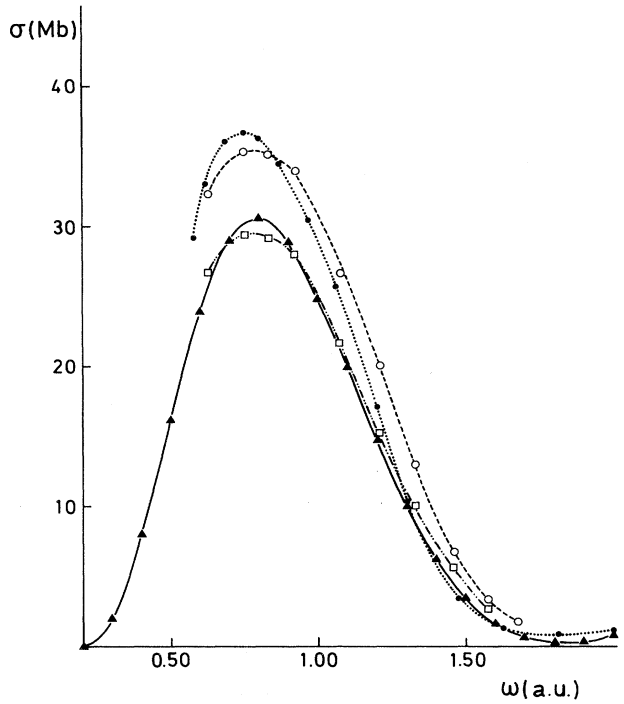

FIG. 4. Computed total photoionization cross section for argon. ▲–▲–▲, present results; ○––○––○, R-matrix results (length form) [27]; □––□––□, R-matrix results (velocity form [27]; ●––●––●, experiment [26].

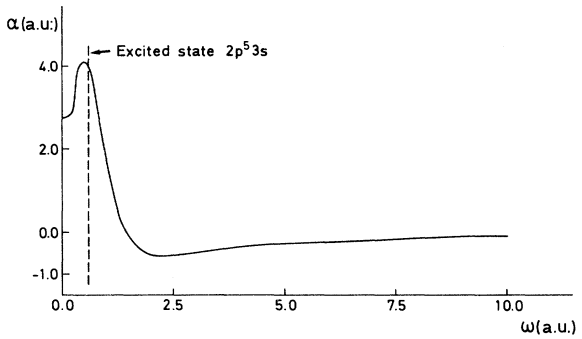

FIG. 5. Dispersion curve [real part of $\alpha(\omega)$ on the real frequency axis] for neon.

the sharp maximum occurring at a photon energy closely below the excitation energy of the first excited state contributing to $\alpha(\omega)$ [cf. Eq. (3)]. Another characteristic feature is the high-frequency behavior which is in reasonable agreement with the free-electron dispersion of $-n/\omega^2$, where n is the number of "free" electrons. The dispersion $\alpha(\omega)$ is related to the index of refraction through Eq. (17).

IV. CONCLUDING REMARKS

The present method to compute atomic and molecular photoionization cross sections depends heavily on a fast convergence of the many-body expansion used to compute the polarizability $\alpha(i\eta)$ on the imaginary frequency axis. The main objective of the present investigation has been to demonstrate the feasibility of the method rather than to seek optimal solutions. Hence the rather unphysical V^N type of potential has been used for practical reasons to obtain the excited one-particle states. Future work will concentrate on applying potentials that are more adapted to describe the potential felt by the outgoing electron from the ionic system left behind.

In the present work the rate of convergence of the many-body expansion is indicated through the disparities between the results obtained with two different partitions of the Hamiltonian (standard and shifted Hamiltonians). In most current works on photoionization the reliability of the predictions is tested by computing "length" as well as "velocity" results. The velocity form is relevant only when matrix elements of the dipole operator between exact eigenstates of the total zero-field Hamiltonian are required. In the present algebraic many-body expansion there is no recourse to exact excited eigenstates, and the velocity form is consequently not relevant.

The inversion of the integral equation [Eq. (15)] is another crucial point. It seems probable that improved accuracy and numerical stability can be achieved by use of a smaller set of more refined basis functions. The algebraic approximation itself with its representation of the continuum through a finite set of one-particle states does not seem to be a serious problem. At least for atoms up to the size of the argon the basis sets can be extended until reasonable saturations are achieved.

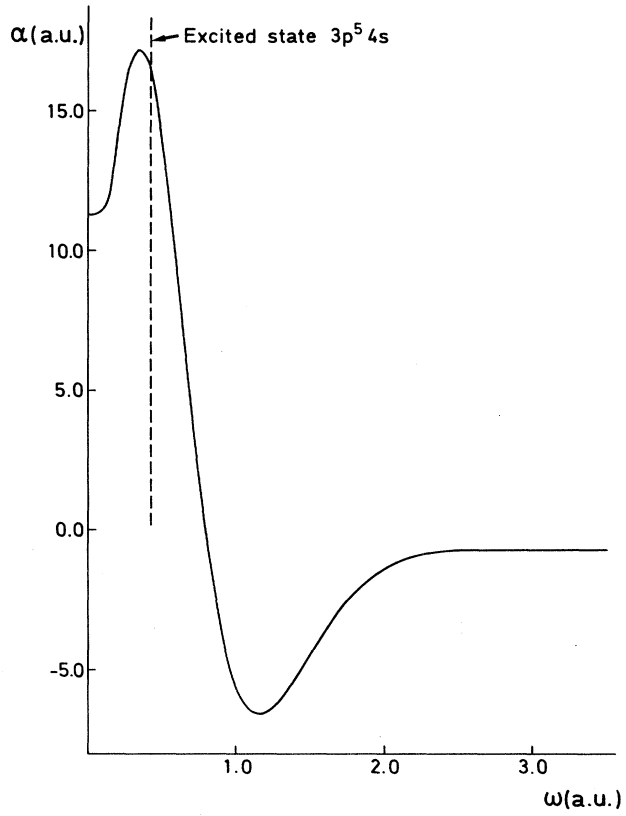

FIG. 6. Dispersion curve for argon.

The present method makes no essential distinction between atoms and molecules. Since there is no explicit recourse to continuum orbitals, there is also no need to invoke the one-center approximation which is standard in current molecular methods. The two examples discussed in the present investigation are both closed-shell atoms. Open-shell systems will, however, not present any new principal problems. The difference will merely be that a series of additional diagrams have to be computed if a many-body expansion for $\alpha(i\eta)$ complete to second order in the Coulomb interaction is to be retained.

Computations have already been carried out for several diatomic molecules, e.g., the first-row hydrides and CO, including openshell systems like CH and OH. The molecular results are planned to be presented in a forthcoming paper.

ACKNOWLEDGMENTS

An initial part of the present work was carried out during a sabbatical stay at the Department of Physics, University of Virginia, Charlottesville. The author is greatly indebted to Professor H. P. Kelly for stimulating discussions and warm hospitality. I also wish to thank Dr. V. Radojevic for helpful contributions. The present work was supported by the U.S. National Science Foundation, and by the Norwegian Research Council for Sciences and the Humanities.

[1] T. E. H. Walker and H. P. Kelly, Chem. Phys. Lett. **16**, 511 (1972).
[2] K. Fagri, Jr. and H. P. Kelly, Phys. Rev. A **23**, 52 (1981).
[3] J. A. Stephens and V. McKoy, J. Chem. Phys. **88**, 1737 (1988).
[4] M. T. Lee, J. A. Stephens, and V. McKoy, J. Chem. Phys. **92**, 536 (1990).
[5] L. Ackermann, A. Görling, and N. Rösch, J. Phys. B **23**, 2485 (1990).
[6] P. W. Langhoff and C. T. Corcoran, J. Chem. Phys. **61**, 146 (1974).
[7] P. W. Langhoff, C. T. Corcoran, J. S. Sims, F. Weinhold, and R. M. Glover, Phys. Rev. A **14**, 1042 (1976).
[8] J. T. Broad and W. P. Reinhardt, Chem. Phys. Lett. **37**, 212 (1976).
[9] I. Cacelli, V. Carravetta, and R. Moccia, J. Phys. B **18**, 1375 (1985).
[10] I. Cacelli, V. Carravetta, and R. Moccia, Mol. Phys. **59**, 385 (1986).
[11] U. Fano and J. W. Cooper, Rev. Mod. Phys. **40**, 441 (1968).
[12] H. P. Kelly, Phys. Rev. **182**, 84 (1969).
[13] N. C. Dutta, T. Ishihara, C. Matsubara, and T. P. Das, Phys. Rev. Lett. **22**, 8 (1969).
[14] S. Wilson, *Electron Correlation in Molecules* (Clarendon, Oxford, 1984).
[15] L. Veseth, J. Phys. B **16**, 2891 (1983).
[16] L. D. Landau and E. M. Lifshitz, *Statistical Physics,* 3rd ed. (Pergamon, Oxford, 1980).
[17] N. Tralli, *Classical Electromagnetic Theory* (McGraw-Hill, New York, 1963).
[18] E. S. Chang, R. T. Pu, and T. P. Das, Phys. Rev. **174**, 16 (1968).
[19] P. M. Morse and H. Feshbach, *Methods of Theoretical Physics* (McGraw-Hill, New York, 1953), Pt. I.
[20] E. Clementi and C. Roetti, At. Data. Nucl. Data Tables **14**, 177 (1974).
[21] A. Kumar and W. J. Meath, Can. J. Chem. **63**, 1616 (1985).
[22] G. Maroulis and A. J. Thakkar, Chem. Phys. Lett. **156**, 87 (1989).
[23] T. M. Miller and B. Bedersen, Adv. At. Mol. Phys. **13**, 1 (1977).
[24] M. Ya. Amusia and N. A. Cherepkov, Case Stud. At. Phys. **5**, 47 (1975).
[25] H. P. Kelly, Phys. Scr. **T17**, 109 (1987).
[26] G. V. Marr and J. B. West, At. Data Nucl. Data Tables **18**, 497 (1976).
[27] P. G. Burke and K. T. Taylor, J. Phys. B **8**, 2620 (1975).
[28] M. Ya. Amusia, N. A. Cherepkov, and L. V. Chernysheva, Zh. Eksp. Teor. Fiz. **60**, 160 (1971) [Sov. Phys.—JETP **33**, 90 (1971)].
[29] H. P. Kelly and R. L. Simons, Phys. Rev. Lett. **30**, 529 (1973).